An Experimental Determination of the Intensity of Friction on the Surface of an Aerofoil.

By A. Fage, A.R.C.Sc., and V. M. Falkner, B.Sc.

(Communicated by L. Bairstow, F.R.S.—Received July 18, 1930.)

[Plate 20.]

Introduction.

1. The principal part of the present investigation* is concerned with an experimental determination of the intensity of friction on the surface of an aerofoil from the well known relation $f = \mu\,(\partial V/\partial z)_{z=0}$, where f is the intensity of friction, μ the coefficient of viscosity, and V the velocity parallel to the surface at a normal distance z from the surface. In general, the velocity changes rapidly near the surface, so that the velocity gradient $(\partial V/\partial z)_{z=0}$ can only be predicted reliably when the velocity observations are taken very close to the surface. A review of the instruments available for the measurement of the velocity very close to a surface led to the conclusion that the most suitable device would be a surface tube of the type designed by Sir Thomas Stanton, and used to examine the conditions at the boundary of a fluid in turbulent motion.† The special feature of this tube is that the inner wall of the tube is formed by the surface itself. Three surface tubes were used in the present experiments, the widths of the openings being 0·0020, 0·0032 and 0·0044 inch respectively. These tubes were calibrated in the known laminar flow in a pipe with a rectangular cross-section, and with them it was possible to measure the velocity at points situated about 2 to 3 thousandths of an inch from the surface. The observations taken with the three tubes were found to be mutually compatible and allowed predictions to be made of the velocity gradients at the surface, and so of the frictional intensities. A check on the general accuracy of these values of frictional intensity was obtained from a comparison of the resultant frictional drag of the aerofoil predicted from them, with that obtained when the form drag

* The work described in this Paper was carried out in the Aerodynamics Department of the National Physical Laboratory, and permission to communicate the results was kindly granted by the Aeronautical Research Committee.

† 'Proc. Roy. Soc.,' A, vol. 97 (1920). By T. E. Stanton, Miss D. Marshall and Mrs. C. N. Bryant.

due to the normal pressures on the surface was subtracted from the total drag deduced from the total head losses in the wake. In addition, explorations of total head in the boundary layer, that is, the thin layer adjacent to the surface throughout which the retarding influence extends, were made with small tubes. It was found that the velocities measured near the surface with these tubes were compatible with those measured still closer to the surface with the surface tubes. The frictional drag of the aerofoil was also determined from the changes of momentum along the boundary layer.*

2. The experiments were made on a large model aerofoil mounted horizontally with very small clearances, between the vertical walls of a 7-foot wind tunnel. The observations were taken midway between the walls, where the flow was closely two-dimensional. To obtain a smooth surface in this region, the middle part (6-inch span) of the model was formed from a hollow gunmetal casting accurately milled to shape and polished. The remainder of the model was a light but stiff wooden framework built up of two longitudinal spars, nose and tail pieces, and transverse ribs, with a hand-finished surface covering of three-ply wood.

The section of the model was symmetrical and of the Joukowski type (see fig. 1). The chord was 39·7 inches and the maximum thickness of the section

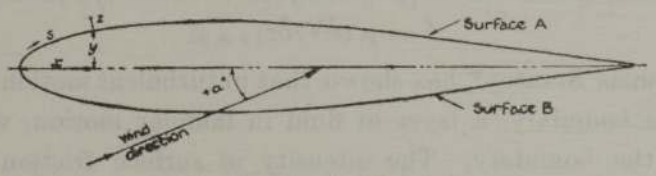

Fig. 1.—Aerofoil Section.

5·98 inches. Details of the construction of the model and also of the shape of the section are given later in § (28) and Table V.

3. *List of Symbols.*

V_0 ≡ Velocity of the undisturbed air stream relative to the model.
V ≡ Velocity at any point in the field.
p_0 ≡ Pressure in the undisturbed air stream.
p ≡ Pressure at any point in the field.
H_0 ≡ Total head in the undisturbed air stream.
H ≡ Total head at any point in the field.

* The observations given in the Paper have not been corrected for the interference of the tunnel walls on the flow around the aerofoil.

$\rho \equiv$ Density of the air.
$\mu \equiv$ Coefficient of viscosity.
$\nu \equiv$ Coefficient of kinematic viscosity.
$K_D \equiv$ Drag coefficient (drag per unit length/$\rho C V_0^2$).
x and $y \equiv$ Co-ordinates of a point on the surface of the aerofoil. The origin is taken at the nose of the section, and the axis OX along the chord.
$z \equiv$ Normal distance of a point from the surface.
$\delta \equiv$ Thickness of the boundary layer, measured normal to the surface.
$s \equiv$ Peripheral distance of a point on the section measured from the nose.
$\bar{z} \equiv$ Distance of the effective centre of a surface tube from the surface.
$C \equiv$ Chord of aerofoil section (39·7 inches).
$A \equiv$ Area.
$f \equiv$ Intensity of surface friction.
$V_1 \equiv$ Mean velocity in calibration pipe.
$W \equiv$ Width of the opening of a surface tube.
$d \equiv$ Depth of the section of the calibration pipe.
$w \equiv$ Width of the section of the calibration pipe.

Determination of the Intensity of Surface Friction (f) from the Relation $f = \mu (\partial V/\partial z)_{z=0}$.

4. Sir Thomas Stanton* has shown that in turbulent motion in pipes there exists at the boundary, a layer of fluid in laminar motion, which has zero velocity at the boundary. The intensity of surface friction f is therefore given by $\mu (\partial V/\partial z)_{z=0}$ where the origin is taken in the boundary, z is measured along the normal, V is the velocity parallel to the boundary, and μ is the coefficient of viscosity of the fluid. This relation can be used to determine the surface friction from the shear in the fluid whether the general motion in the boundary layer is laminar or turbulent.

5. *Surface Tubes.*—It is apparent that to determine the value of $(\partial V/\partial z)_{z=0}$ it is essential to take measurements of velocity very close to the surface. To allow this to be done, Sir Thomas Stanton designed a special form of Pitot tube, which was such that the inner wall of the tube was formed by the surface itself, and for which the width of the opening could be varied by moving the outer wall. Tubes of a somewhat similar type have been used in the present experiments. A departure in design had, however, to be made, for since numerous observations had to be taken at different points on the surface,

* *Loc. cit.*

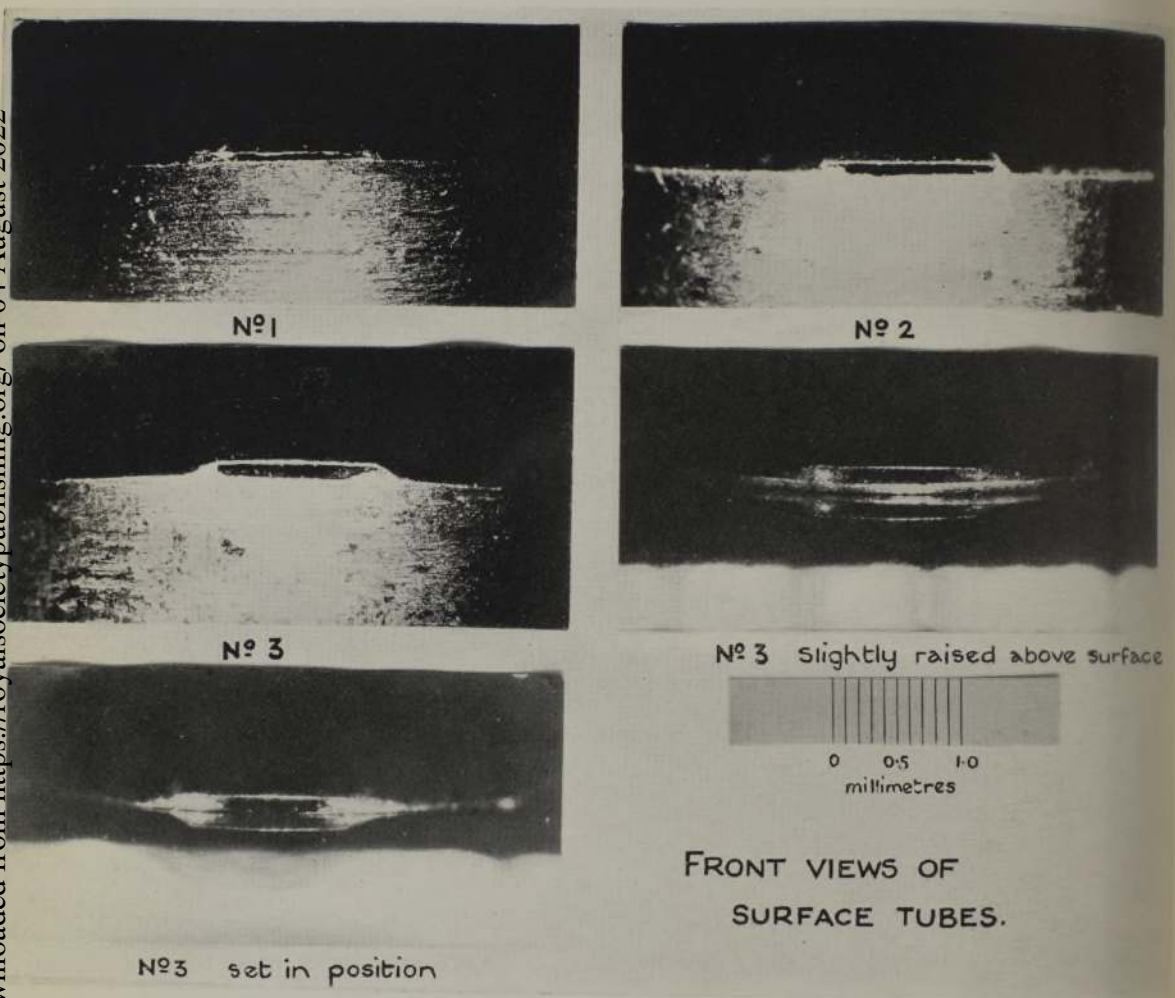

FIG. 3.

(*Facing p.* 381.)

the labour involved in fitting a tube for which the opening could be varied at will would be excessive. It was decided therefore to use several tubes with very small fixed openings, each tube being constructed on the top of a circular rod of diameter 0·2 inch, designed to pass with a very small clearance through holes in the surface of the model, and to mount each tube so that the top surface of the rod was flush with the surface of the model. Three tubes of this type—designated hereinafter Surface Tubes Nos. 1, 2 and 3—were constructed, the widths of the openings being 0·0020, 0·0032, and 0·0044 inch respectively. The outer wall of each tube was formed by a thin steel cap, rectangular in plan form, ground at the front edge to a thickness of about 0·0006 inch. A hole of fine bore drilled along the axis of the rod served to transmit the pressure at the mouth of a tube to the manometer.

6. Great care was taken in setting a surface tube. The method of setting is illustrated in the diagrammatic sketch of fig. 2. A small reflecting glass

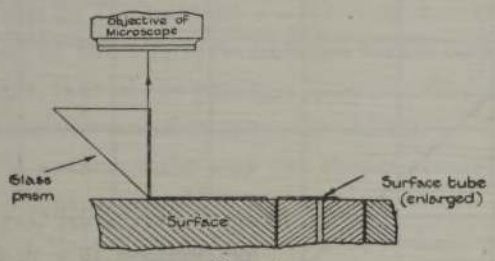

Fig. 2.

prism with a sharp edge in contact with the surface was used as a mirror to light along the surface. The image obtained was viewed under a microscope (magnification 40). At the outset, the carrier rod was slowly lowered until its top surface was just above the surface of the aerofoil. The rod was then tapped until its front edge just disappeared. The top of the rod, and so the inner wall of the tube, was then flush with the surface. A check on the accuracy of mounting was obtained from a measurement of the width of the tube opening on a graticule carried in the eyepiece of the microscope. To obtain a clear image a beam of light from a Pointolite lamp was focussed on to the mouth of a tube. Two of the photographs in fig. 3 (Plate 20) show a tube just raised above the surface and also just mounted in place.* Photographs of the mouths of the three tubes are also shown. The device, mounted within the aerofoil, which held a surface tube in place is described later in § (20). This method of setting a surface tube was found to work satisfactorily in practice.

* Reflected images in the bright surface are also seen.

7. *Calibration of Tubes.*—It is known that when the opening of a surface tube is very small, the speed deduced from the pressure at the mouth is not the same as that at the geometrical centre of the opening. Each tube had therefore to be calibrated to determine the position of the " effective centre," corresponding to the speed deduced from the measured pressure. These calibrations were made in a long pipe of rectangular cross-section, which had laminar flow at the cross-section where a tube was placed. The mean flow and the velocity distribution at the wall were calculated from the measured pressure drop down the pipe. The information needed for the design of the calibration pipe was obtained from a paper by S. J. Davies and C. M. White,* on an experimental study of the flow of water in pipes of rectangular section. The relevant data taken from that paper are given in the curves of fig. 4.

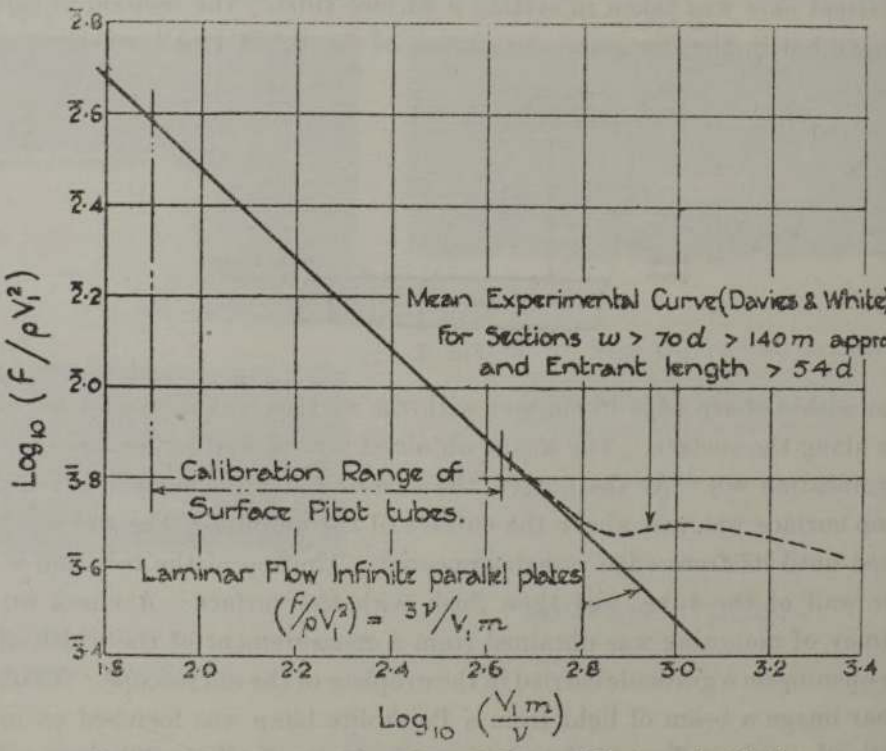

Fig. 4.—Resistance to Flow through Pipes of Rectangular Section.

They show that when the ratio of the width (w) to the depth (d) of the cross-section of a rectangular pipe exceeds 70, the coefficient of frictional resistance at a distance from the mouth greater than 54 d has the same value as that for the laminar flow between infinite parallel plates at the distance (d) apart, provided

* 'Proc. Roy. Soc.,' A, vol. 119 (1928).

the value of (mV_1/ν) does not exceed 450 ($[\log_{10}(mV_1/\nu) = 2{\cdot}65]$), where m is the hydraulic mean depth, that is the area of the section divided by the periphery, and V_1 is the mean rate of flow in the pipe.

8. The dimensions of the pipe used for the calibration of the surface tubes were :—Overall length 17·0 inches, width of the section 1·97 inches, depth of the section 0·0300 inch. Each tube was mounted on the centre line of one of the wider walls at a distance of 10 inches (entrant length 330 d), from the mouth, and calibrated over a speed range 10 to 54 ft./sec. [$\log_{10}(V_1m/\nu) =$ 1·9 to 2·63.] The conditions necessary for laminar flow were therefore satisfied, and the flow between the two wider walls could be taken as the same as the laminar flow between parallel plates of infinite extent at the distance apart. The mean rate of flow down the pipe was therefore given by the expression $V_1 = f\,d/6\mu = (d^2/12\mu)\ \partial p/\partial l$, where $(\partial p/\partial l)$ was the pressure gradient down the pipe ; and the distance $\bar{z}$ from the wall corresponding to a velocity V was given by the relation $\bar{z} = [1 - \sqrt{1 - (2V/3V_1)}]\,.\,d/2$.

The determination of the effective distance $\bar{z}$ involved therefore only two measurements. First, that of the pressure drop $(\partial p/\partial l)$ from which the mean velocity V_1 was estimated ; and, second, the difference between the pressure at the mouth of the surface tube and the static pressure in the pipe, from which the velocity V was deduced.

It should be added that a part (of length 12 inches) of the wall on which the tube was mounted was made detachable, to facilitate the mounting of the tube : that the air was sucked through the pipe by a centrifugal blower of the ordinary type : and that a few velocity observations taken with a small Pitot tube at the centre of the pipe were found to be in reasonably close agreement with those predicted from the pressure drop on the assumption that the flow was laminar.

9. The results obtained from several calibrations of each surface tube are given in fig. 5. Values taken from the curves in this figure are also collected in Table I, in a form which readily reveals some interesting characteristics of these tubes. Reference to this table shows that the effective centre of Tube No. 3 was within the opening and just beyond its geometrical centre, whereas the effective centre of Tube No. 1 was beyond the outer edge of the opening. The ratio of the effective distance $\bar{z}$ to the width of the opening W increased therefore as the width was decreased.* Table I also shows that there was a pronounced outward movement of the effective centre of each tube, as the speed at the mouth was decreased. But the most important

* See Stanton, *loc. cit.*

Table I.—W ≡ Width of the Opening of a Tube.

Velocity calculated from the pressure at the mouth of the tube. V ft./sec.	Value of $\bar{z}$ (inches).		
	No. 3. W = 0·0044 inch (mean values).	No. 2. W = 0·0032 inch. Curve E.	No. 1. W = 0·0020 inch (mean values).
8	0·00320	0·00320	0·00270
11	0·00298	0·00296	0·00253
14	0·00281	0·00276	0·00238
17	0·00268	0·00258	0·00224
20	0·00255	0·00241	0·00217

characteristic exhibited in Table I, in so far as the present work was concerned, was that although the opening of Tube No. 1 was less than one-half of that of Tube No. 3, yet the effective distance was only about 15 per cent. smaller. Tube No. 1 with its smaller opening did not, therefore, allow observations to be taken much closer to the surface than either of the Tubes Nos. 2 and 3. Tube No. 1 was used to a very limited extent on the aerofoil.

In view of the tendency for the mouth of a tube to become partially blocked with fine dust, it was necessary on occasions to clean out the mouth, and, whenever this was done, the tube was re-calibrated. The results of these calibrations, and also the dates at which they were made, are given in fig. 5. The curves for Tube No. 3 show systematic changes with time ; and it is not improbable that these changes are connected with small alterations in the shape of the mouth which occurred when it was cleaned.

The relatively large differences between the calibration curve E for Tube No. 2 and the curves F and G taken at earlier dates arise however from another cause. After this tube has been in use for some time a very small leak was discovered at an edge of the outer wall, and after this edge had been coated with " Newskin," the upper curve E was obtained. There was, however, no need to discard the observations taken on the aerofoil with this tube before the discovery of the leak, for the appropriate calibration of the tube for its condition at the time of observation was used to estimate the velocity at the surface. It may be concluded, however, that the curves given in fig. 5 clearly illustrate the need for frequent calibrations of this type of small surface tube.

Some values taken from the calibration curves obtained by Sir Thomas Stanton for a surface tube with a movable outer wall are plotted in fig. 5. These have the same character as those obtained for the tubes used in the

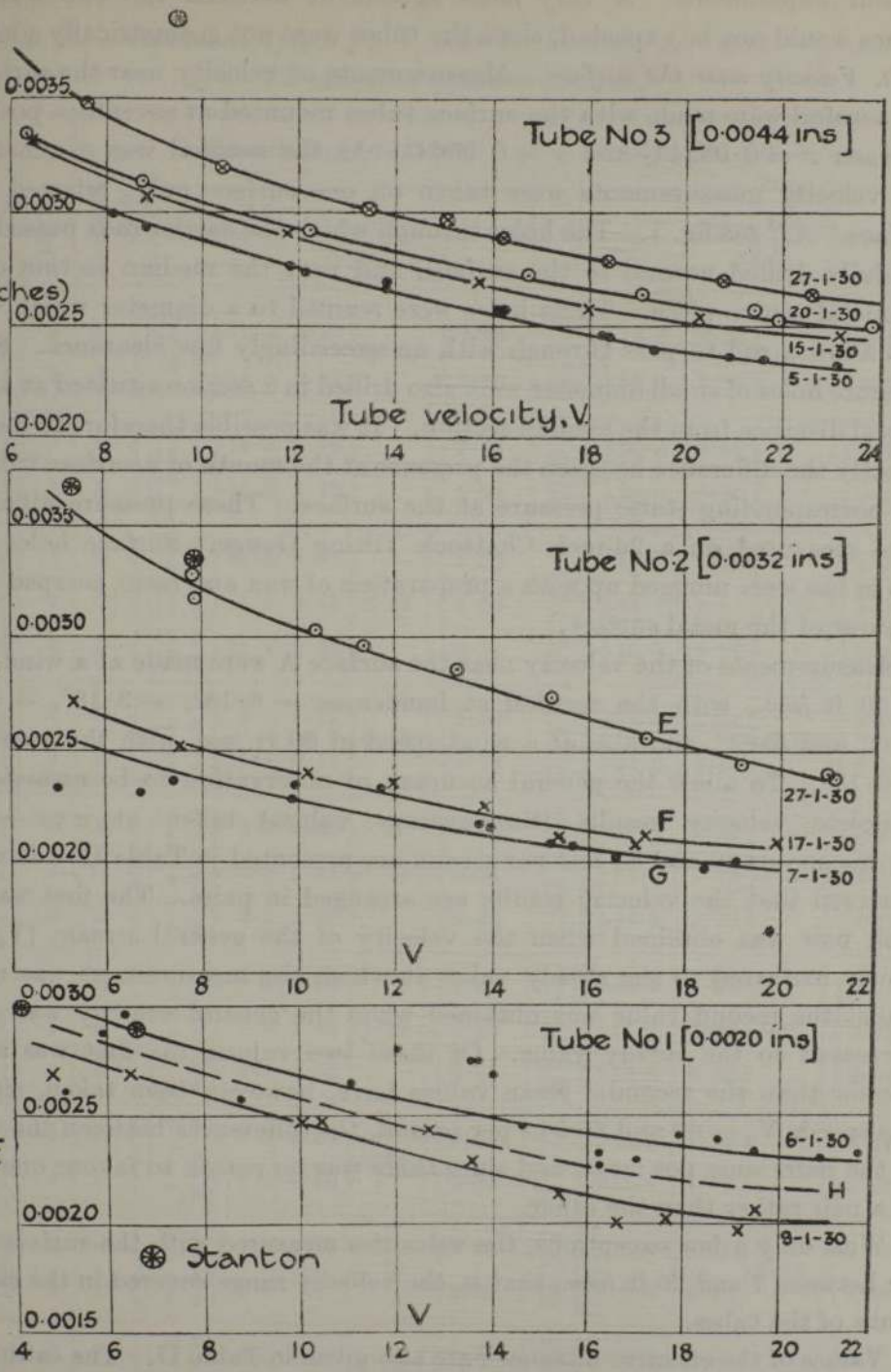

FIG. 5.

present experiments. A very close agreement between the two series of values would not be expected, since the tubes were not geometrically similar.

10. *Velocity near the surface.*—Measurements of velocity near the surface of the aerofoil were made with the surface tubes mounted at seventeen positions between $x = 0{\cdot}0524$ C and $x = 0{\cdot}956$ C. As the aerofoil was symmetrical, the velocity measurements were taken on one surface only, referred to as surface "A," see fig. 1. The holes through which the carrier rods passed were carefully drilled normal to the surface, and near the median section of the gunmetal centre piece. These holes were reamed to a diameter which would just allow a rod to pass through with an exceedingly fine clearance. Static-pressure holes of small diameter were also drilled in a section situated at a small lateral distance from the median section. It was possible therefore to measure directly the difference between the pressure at the mouth of a surface tube and the corresponding static pressure at the surface. These pressure differences were measured on a 26-inch Chattock Tilting Gauge. Surface holes when not in use were plugged up with a preparation of wax and resin, scraped to the contour of the metal surface.

Measurements of the velocity near the surface A were made at a wind speed of 60 ft./sec., with the aerofoil at incidences $-6{\cdot}18°$, $-3{\cdot}18°$, $-0{\cdot}18°$, $2{\cdot}82°$ and $5{\cdot}82°$, and also at a wind speed of 80 ft./sec. with the aerofoil at $-0{\cdot}18°$. To allow the general accuracy of observation to be assessed, the complete velocity results (time-average values) taken at $\alpha = -0{\cdot}18°$ for the speeds 60 and 80 feet per second are presented in Table II. It will be observed that the velocity results are arranged in pairs. The first value of each pair was obtained when the velocity of the general stream (V_0) was slowly increased to the steady value at which the measurement was made; whilst the second value was obtained when the general velocity was slowly decreased to the steady value. Of these two values, the first was always greater than the second. Mean values have, however, been taken, since at the speeds $V_0 = 60$ and 80 feet per second, the differences between the values of the pairs were not large, and since there was no reason to favour one value of a pair rather than the other.

With only a few exceptions, the velocities measured with the surface tubes lie between 7 and 20 ft./sec., that is, the velocity range covered in the calibrations of the tubes.

Values of the effective distance $\bar{z}$ are also given in Table II. The calibration curve of fig. 5, selected for the determination of $\bar{z}$, was the one taken at the date nearest to that at which the velocity measurements were made on the

Table II.—Values of $(f/\rho V_0^2)$, V, and $\bar{z}$. Surface A. $a = -0{\cdot}18°$.
$\bar{z} \equiv$ effective distance (inches).

(x/c).	Tube.	Calibration Curve.	Velocity, $V_0 = 60$ ft./sec.			Velocity, $V_0 = 80$ ft./sec.		
			V, ft./sec.	$\frac{(f \times 10^3)}{\rho V_0^2}$.	$(\bar{z} \times 10^3)$.	V, ft./sec.	$\frac{(f \times 10^3)}{\rho V_0^2}$.	$(\bar{z} \times 10^3)$.
0·0167	2	E	13·0, 12·2 → 12·6	2·37 } 2·38	2·86	18·6, 18·3 → 18·5	2·24 } 2·22	2·49
	3	A	13·7, 13·4 → 13·5	2·39	3·03	19·9, 19·8 → 19·9	2·20	2·73
0·0330	2	E	14·3, 13·7 → 14·0	2·72 } 2·75	2·76	20·6, 20·2 → 20·4	2·58 } 2·54	2·39
	3	A	15·3, 15·1 → 15·2	2·77	2·94	21·9, 22·1 → 22·0	2·50	2·66
0·0504	1	H	11·2, 9·6 → 10·4	2·17	2·56	16·0, — → 16·0	2·12	2·28
	2	G	12·4, 11·2 → 11·8	2·88 } 2·53	2·20	18·0, 17·4 → 17·7	2·67 } 2·39	2·00
	3	D	12·8, 12·8 → 12·8	2·54	2·71	18·8, 19·2 → 19·0	2·37	2·42
0·0756	2	G	10·5, 8·5 → 9·5	2·21 } 2·19	2·30	14·8, 14·4 → 14·6	2·11 } 2·13	2·08
	3	D	12·4, 10·2 → 11·3	2·17	2·79	18·0, 17·2 → 17·6	2·14	2·48
0·1007	1	H	11·2, 8·2 → 9·7	2·00	2·60	15·3, 14·7 → 15·0	1·95	2·32
	2	G	9·9, 8·1 → 9·0	2·07 } 1·96	2·32	13·7, 12·9 → 13·3	1·87 } 1·84	2·14
	3	D	10·1, 9·3 → 9·7	1·80	2·89	14·8, 14·8 → 14·8	1·70	2·62
0·1511	1	H	10·1, 7·9 → 9·0	1·83	2·64	15·3, 14·5 → 14·9	1·94	2 32
	2	G	9·2, 5·8 → 7·5	1·69 } 1·69	2·40	11·8, 10·6 → 11·2	1·36 } 1·61	2·22
	3	D	8·8, 8·4 → 8·6	1·56	2·96	13·5, 13·5 → 13·5	1·52	2·68
0·2015	2	G	7·9, 7·1 → 7·5	1·68 } 1·54	2·40	13·7, 13·3 → 13·5	1·90 } 1·79	2·14
	3	D	8·2, 7·6 → 7·9	1·40	3·02	14·9, 14·3 → 14·6	1·68	2·63
0·252	2	G	8·2, 7·2 → 7·7	1·73 } 1·67	2·39	16·7, 15·9 → 16·3	2·41 } 2·33	2·04
	3	D	9·0, 8·8 → 8·9	1·61	2·95	18·3, 18·3 → 18·3	2·24	2·46
0·302	2	F	9·4, 8·6 → 9·0	1·97 } 1·92	2·45	19·2, 19·2 → 19·2	2·80 } 2·74	2·07
	3	C	10·4, 10·2 → 10·3	1·86	2·98	21·9, 22·1 → 22·0	2·68	2·48

Table II—(continued).

(x/c).	Tube.	Calibration Curve.	Velocity, $V_0 = 60$ ft./sec.			Velocity, $V_0 = 80$ ft./ sec.		
			V, ft./sec.	$\frac{(f \times 10^3)}{\rho V_0^2}$.	$(\bar{z} \times 10^3)$.	V, ft./sec.	$\frac{(f \times 10^3)}{\rho V_0^2}$.	$(\bar{z} \times 10^3)$.
0·353	2	F	12·3 11·5 } 11·9	2·77 } 2·73	2·30	22·6 22·2 } 22·4	3·34 } 3·29	2·02
	3	C	14·1 13·7 } 13·9	2·69	2·77	26·1 25·9 } 26·0	3·24	2·42
0·403	2	F	13·4 12·2 } 12·8	3·05 } 2·93	2·26	22·5 21·9 } 22·2	3·29 } 3·20	2·04
	3	C	14·5 14·3 } 14·4	2·81	2·75	25·1 24·9 } 25·0	3·11	2·43
0·504	2	F	13·1 12·1 } 12·6	3·05 } 2·85	2·21	19·3 19·1 } 19·2	2·80 } 2·66	2·07
	3	C	13·8 13·8 } 13·8	2·65	2·79	20·8 21·0 } 20·9	2·52	2·50
0·605	2	F	12·0 11·2 } 11·6	2·70 } 2·61	2·31	16·8 16·6 } 16·7	2·38 } 2·34	2·12
	3	C	13·3 13·1 } 13·2	2·52	2·81	19·4 19·4 } 19·4	2·30	2·54
0·706	2	F	11·4 10·2 } 10·8	2·46 } 2·39	2·35	16·5 16·1 } 16·3	2·32 } 2·23	2·13
	3	C	12·6 12·2 } 12·4	2·32	2·86	18·4 18·4 } 18·4	2·15	2·59
0·807	2	F	7·7 6·9 } 7·3	1·54 } 1·62	2·56	11·7 11·7 } 11·7	1·53 } 1·55	2·30
	3	B	10·0 9·6 } 9·8	1·70	3·07	14·6 14·6 } 14·6	1·57	2·80
0·868	2	F	7·5 6·5 } 7·0	1·46 } 1·54	2·58	11·6 10·8 } 11·2	1·44 } 1·46	2·35
	3	B	9·5 9·3 } 9·4	1·62	3·10	13·9 13·9 } 13·9	1·47	2·84
0·956	3	A	8·1 7·5 } 7·8	1·22	3·45	11·9 13·9 } 12·9	1·27	3·06

The first value of V was measured when the tunnel speed was slowly increased to its steady value ; and the second value when the tunnel speed was slowly decreased to its steady value.

aerofoil. The values of $\bar{z}$ are seen to be very small, and almost all of them lie between 2 and 3 thousandths of an inch.

It should be added that experiments were made at the tunnel speeds of 60 and 80 feet per second only, because the definite impression was formed that reliable accuracy would only be obtained with a small surface tube, when the pressure to be measured was not too small.

11. *The intensity of surface friction.*—It has just been shown that measure-

ments of velocity have been made very near the surface at normal distances $\bar{z}$ of 2 to 3 thousandths of an inch. The intensity of surface friction has been estimated from these results on the assumption that the velocity increases linearly from the zero value at the surface to the value V measured at the small distance $\bar{z}$. The intensity of surface friction is then given by the relation $f = \mu(V/\bar{z})$. Evidence will be given later to show that this assumption of linearity cannot be very far from the truth. The value of μ taken was $3{\cdot}82 \times 10^{-7}$ (slug-feet sec. units), which was the mean value for the temperature range (19·5° C. to 22·5° C.) covered in the experiments.

The values of $(f/\rho V_0^2)$ estimated from the velocity observations taken on the aerofoil at $-0{\cdot}18°$ incidence are given in Table II. An examination of these results shows that the values for Tube No. 2 tended to be slightly greater than those for Tube No. 3, but in general the agreement between the two series of values was close; and also that the few values for Tube No. 1 did not greatly differ from those for either Tube No. 2 or Tube No. 3. Accordingly, the means of the values of $(f/\rho V_0^2)$ for the three tubes were taken. Except in a few cases, an individual value differed from its mean value by less than $\pm$ 6 per cent.

12. The distributions of surface friction over surface A at incidences $-6{\cdot}18°$, $-3{\cdot}18°$, $-0{\cdot}18°$, $2{\cdot}82°$ and $5{\cdot}82°$ are shown in figs. 6–8. It will be noticed (see fig. 1) that since the section is symmetrical the frictional curves measured on surface A at a negative incidence can be taken as those for the under surface of the aerofoil at a positive incidence. The curves in fig. 7 do not therefore differ greatly from those for the upper and under surfaces of the aerofoil at 3°. The experiments were in fact conducted at nominal incidences of $\pm 3°$, but a correction of $-0{\cdot}18°$ had to be applied afterwards. Similarly the curves in fig. 8 are not greatly different from those for the upper and under surfaces of the aerofoil at an incidence of 6°.

Reference to figs. 6–8 shows that the frictional curves for the upper surface (surface A at a positive incidence) have two maxima, one situated near the nose and the other, a greater one, some distance beyond the first. As the incidence is increased both maxima become greater and they move towards the nose. The curves for the under surface (surface A at a negative incidence) also have two maxima, but they are smaller than those for the upper surface and move towards the tail as the incidence is increased. Measurements of the velocity distribution in the boundary layer (see later) suggest that a transition from laminar to turbulent flow takes place in the part of the boundary layer situated between the two maxima. The first maximum is therefore

associated with laminar flow, and the second with turbulent flow in the boundary layer. It must, however, be mentioned that it was noticed when taking observations of pressure at the nose of the aerofoil that the motion

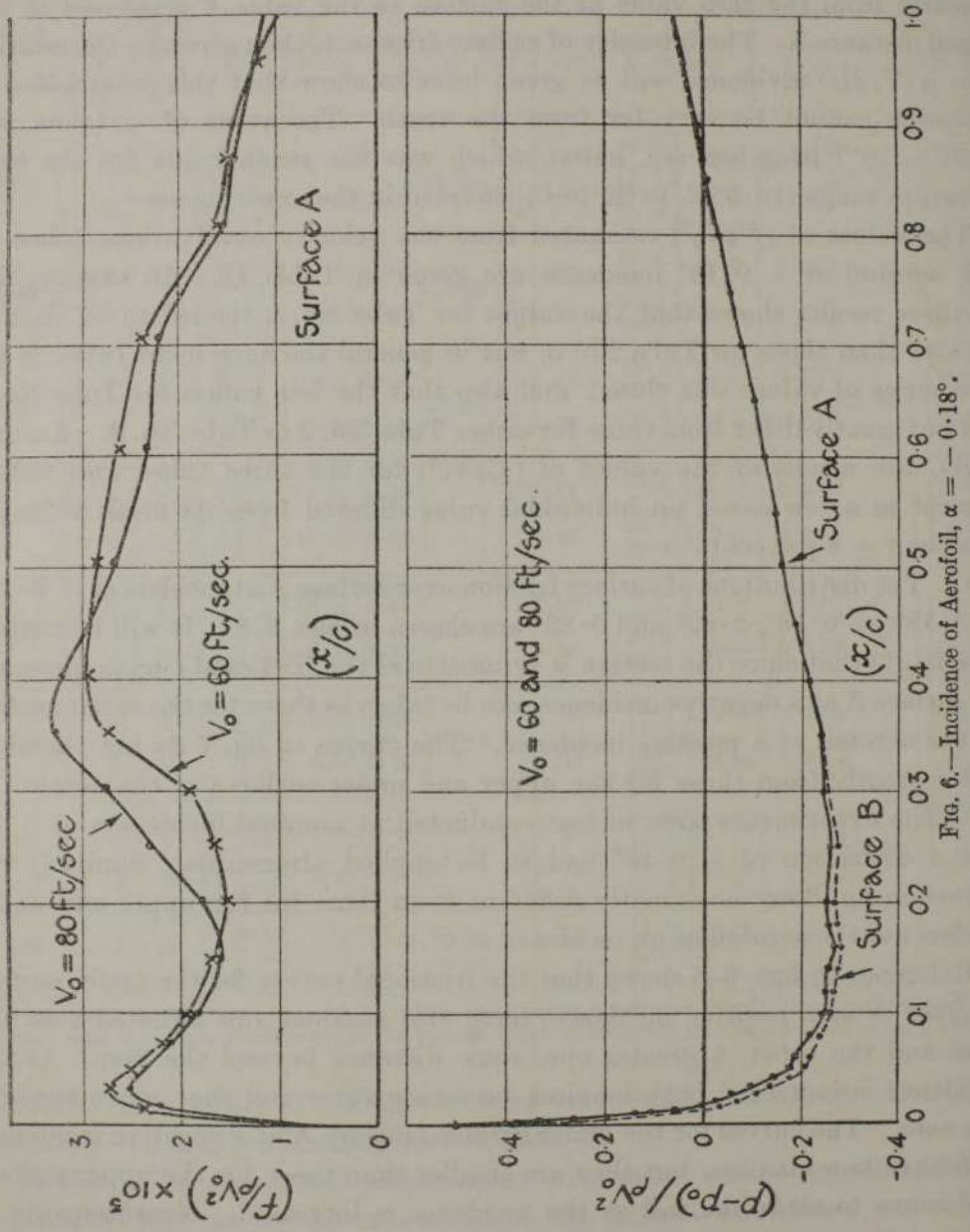

FIG. 6.—Incidence of Aerofoil, $\alpha = -0{\cdot}18°$.

was disturbed, and it is doubtful whether in this limited region the flow was laminar.

Another feature exhibited in the figs. 6–8 is that beyond the second maxi-

mum, on either the upper or the lower surface, the frictional intensity steadily falls with the distance from the nose. The frictional intensity does not,

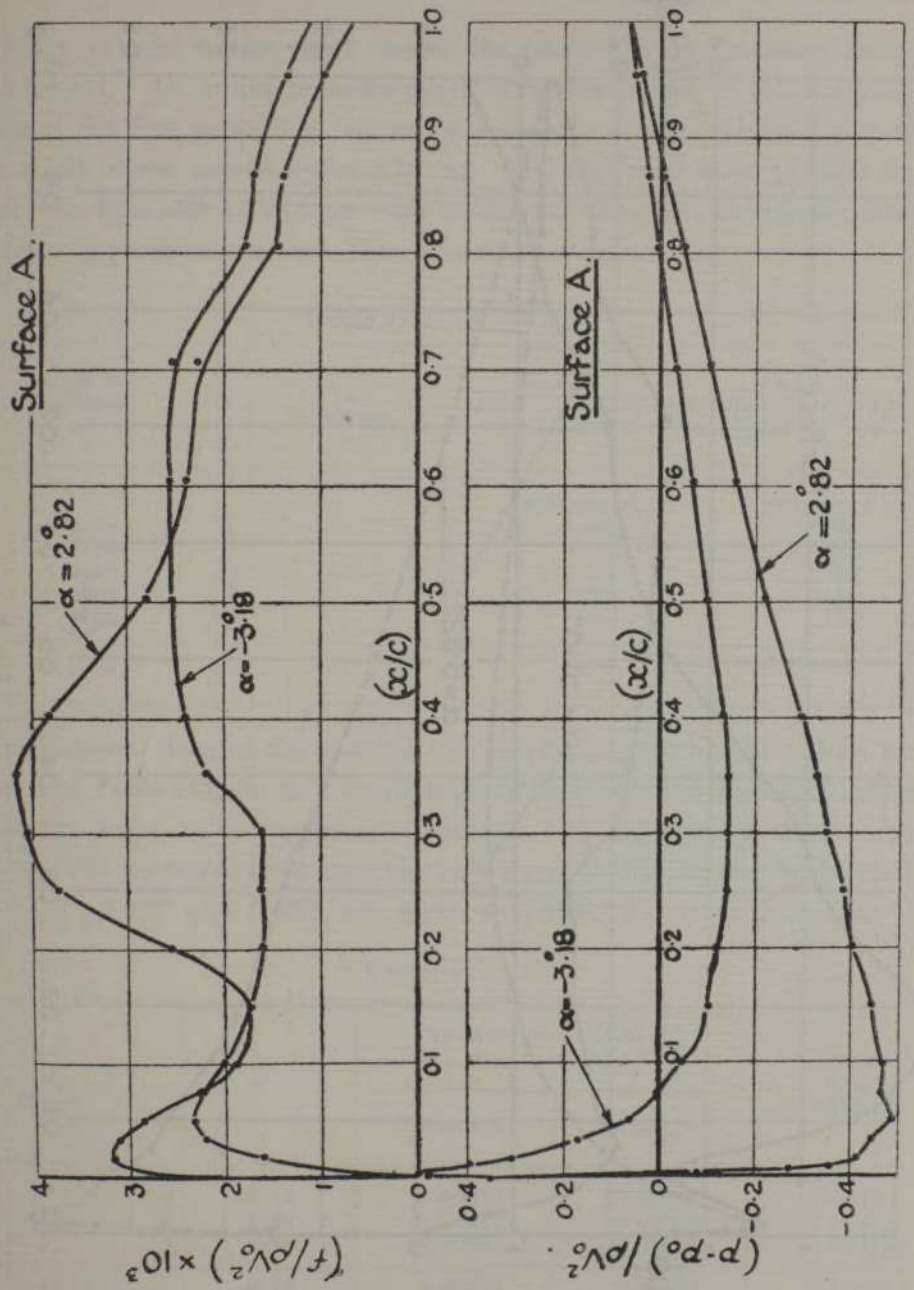

FIG. 7.

however, fall to zero on any part of the surface, even on the tail of the aerofoil at 5·82° incidence.

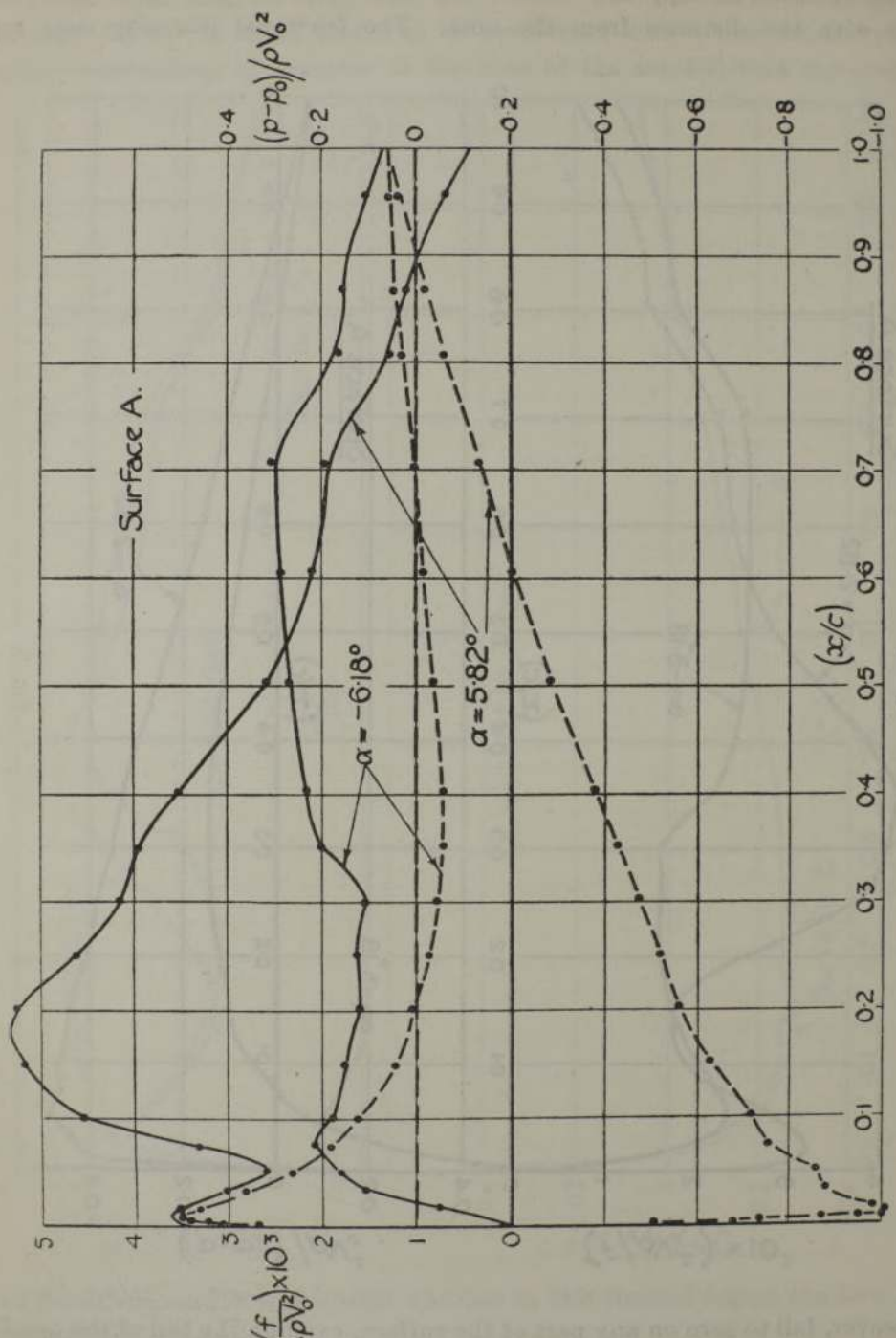

FIG. 8.

13. Values of $\int_{x=0}^{x=C} (f/\rho V_0^2 C)\, ds$, that is the integral taken over the surface of the frictional intensities, and also of $\int_{x=0}^{x=C} (f/\rho V_0^2 C)\, dx$, that is the force parallel to the chord due to the friction on the surface, are given in Table III. As would be anticipated from the shape of the surface, the values of the first series (Col. *a*) are only slightly greater (about 2 per cent.) than those of the second series (Col. *b*). The frictional force parallel to the chord (Col. *b*) is seen to increase with incidence. The rate of increase is much greater at a positive incidence than at a negative incidence.

Table III.—*Surface A.*

Angle of Incidence. $\alpha°$.	V_0 ft. per sec.	$10^3 \int_{x=0}^{x=C} (f/\rho V_0^2 C) ds$.	$10^3 \int_{x=0}^{x=C} (f/\rho V_0^2 C)\, dx$.
		(Column *a*.)	(Column *b*.)
−6·18	60	1·97	1·96
−3·18	60	2·06	2·02
−0·18	60	2·15	2·10
2·82	60	2·50	2·45
5·82	60	2·81	2·79
−0·18	80	2·20	2·16

The frictional drag of the aerofoil can be predicted from the values given in Col. *b* of Table III, for at a small angle of incidence the frictional drag has almost the same value as the frictional force acting parallel to the chord. Values of the frictional drag coefficient obtained in this manner for incidences of −0·18°, 2·82° and 5·82°, are given in Table IV. It is there seen that

Table IV.

V_0 ft./sec.	$\alpha°$	Contribution to frictional drag coefficient.		Frictional drag coefficient.
		Surface A.	Surface B.*	
60	−0·18	0·00210	0·00215	0·00425
60	2·82	0·00245	0·00205	0·00450
60	5·82	0·00280	0·00195	0·00475
80	−0·18	0·00215	0·00220	0·00435

* These values were obtained by interpolation from the values for Surface A at a negative incidence.

the frictional drag coefficient increases slowly with incidence from 0·00425 at $\alpha = -0{\cdot}18°$ to 0·00475 at $\alpha = 5{\cdot}82°$; and also that the upper surface makes a greater fractional contribution to the frictional drag of the aerofoil, as the incidence is increased.

Measurement of the frictional drag of the aerofoil at $\alpha = -0{\cdot}18°$.

14. It is known that the frictional drag of an aerofoil can be determined by subtracting the form drag, that is the drag due to the normal pressures on the surface, from the total drag. An estimate of the frictional drag of the aerofoil at $\alpha = -0{\cdot}18°$ has been obtained in this manner, and compared with that predicted from the frictional intensities ($f/\rho V_0^2$) given in Table II.

15. *Total drag.*—The total drag was estimated from the integral of the total-head losses measured in the wake behind the median section of the metal centre piece. This method was used in preference to that of direct measurement, because the latter method would have involved the measurement of the drag of the composite model, with wooden and metal surfaces of different texture, whereas it was the drag of that part of the model with the metal surface that was needed. It was also known from some earlier experiments* that the results obtained by the total-head method would be in close agreement with those obtained by direct measurement.

The total-head losses were estimated from explorations of total head taken along lines normal to the undisturbed stream and situated at distances 1·1 C. behind the trailing edge, and 0·6 C. in front of the leading edge of the aerofoil. Curves of the total-head losses are given in fig. 9. The values of K_D determined from the areas of these diagrams are given on the diagrams. The drag coefficient of the aerofoil at an incidence of $-0{\cdot}18°$ is seen to be 0·0054.†

16. *Pressure experiments.*—Experiments were undertaken to measure the pressure distributions (*a*) around a section of the aerofoil at an incidence of $-0{\cdot}18°$, for the speeds 60 and 80 ft./sec.; and (*b*) over the surface A at incidences of $-6{\cdot}18°$, $-3{\cdot}18°$, $-0{\cdot}18°$ (a repeat measurement), $2{\cdot}82°$ and $5{\cdot}82°$, for the wind speed 60 ft./sec. In experiments (*a*), the pressure was measured at 39 holes drilled through the upper surface and the same number through the lower surface. In experiments (*b*), the pressure was measured at the 17 holes used in the experiments of §10, and in addition at the first

* Experiments on a Series of Symmetrical Joukowski Sections. By Fage, Falkner and Walker. Aeronautical Research Committee, R. and M. 1241 (Table II).

† The drag coefficient in an infinite stream would be about 0·0052; see R. and M. 1241.

10 holes (at the nose) used in experiments (*a*). The pressure at each hole was measured on a 26-inch Chattock Tilting Gauge against the static pressure (p_0) in the undisturbed wind. The experiments were made at nominal

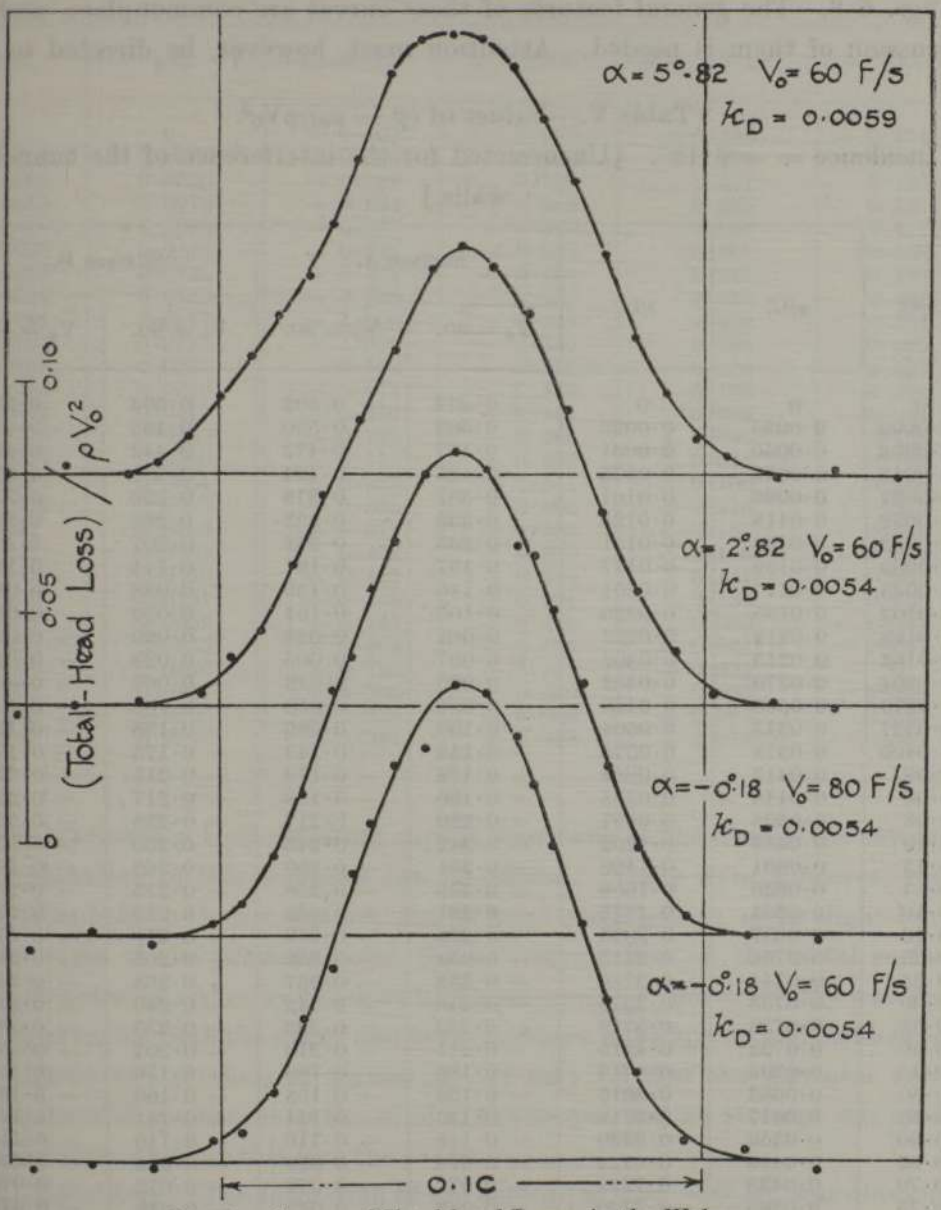

FIG. 9.—Curves of Total-head Losses in the Wake.

incidences of $-6°$, $-3°$, $0°$, $3°$ and $6°$. An analysis of all the pressure observations showed that at a nominal incidence of 0°, the true incidence was $-0{\cdot}18°$. This correction was therefore applied to the nominal values of incidence.

The pressure results from the two series of experiments, expressed as non-dimensional coefficients $(p - p_0)/\rho V_0^2$, are collected in Tables V and VI. The curves obtained by plotting values of $(p - p_0)/\rho V_0^2$ against x/C are given in figs. 6–8. The general features of these curves are commonplace, and no discussion of them is needed. Attention must, however, be directed to the

Table V.—Values of $(p - p_0)/\rho V_0^2$.

Incidence $= -0{\cdot}18°$. [Uncorrected for the interference of the tunnel walls.]

x/C.	y/C.	s/C.	Surface A.		Surface B.	
			$V_0 = 60$.	$V_0 = 80$.	$V_0 = 60$.	$V_0 = 80$.
0	0	0	0·504	0·502	0·504	0·503
0·0002	0·0025	0·0025	0·503	0·500	0·485	0·487
0·0008	0·0050	0·0051	0·477	0·472	0·442	0·438
0·0015	0·0073	0·0075	0·425	0·424	0·380	0·377
0·0027	0·0096	0·0101	0·381	0·378	0·326	0·326
0·0039	0·0118	0·0126	0·332	0·333	0·268	0·268
0·0053	0·0139	0·0151	0·265	0·262	0·207	0·206
0·0069	0·0159	0·0177	0·197	0·197	0·144	0·141
0·0085	0·0177	0·0201	0·140	0·139	0·088	0·083
0·0103	0·0195	0·0226	0·105	0·104	0·050	0·050
0·0123	0·0212	0·0252	0·061	0·059	+ 0·020	+ 0·021
0·0162	0·0243	0·0302	+ 0·007	+ 0·005	− 0·028	− 0·029
0·0204	0·0270	0·0352	− 0·020	− 0·022	− 0·069	− 0·066
0·0270	0·0308	0·0428	− 0·058	− 0·058	− 0·108	− 0·107
0·0337	0·0343	0·0504	− 0·100	− 0·099	− 0·138	− 0·141
0·0405	0·0375	0·0578	− 0·143	− 0·143	− 0·175	− 0·174
0·05	0·0413	0·0682	− 0·178	− 0·179	− 0·211	− 0·211
0·06	0·0448	0·0788	− 0·186	− 0·188	− 0·217	− 0·219
0·08	0·0508	0·0997	− 0·220	− 0·217	− 0·236	− 0·237
0·10	0·0559	0·1202	− 0·242	− 0·243	− 0·255	− 0·257
0·12	0·0601	0·1406	− 0·251	− 0·250	− 0·266	− 0·266
0·14	0·0636	0·1609	− 0·258	− 0·258	− 0·275	− 0·274
0·16	0·0664	0·1812	− 0·261	− 0·262	− 0·279	− 0·278
0·18	0·0687	0·2015	− 0·258	− 0·259	− 0·271	− 0·270
0·20	0·0706	0·2215	− 0·254	− 0·250	− 0·265	− 0·262
0·25	0·0741	0·2715	− 0·258	− 0·257	− 0·268	− 0·267
0·30	0·0753	0·3215	− 0·246	− 0·242	− 0·249	− 0·246
0·35	0·0750	0·3715	− 0·233	− 0·233	− 0·235	− 0·236
0·40	0·0733	0·4215	− 0·211	− 0·210	− 0·207	− 0·206
0·45	0·0702	0·4715	− 0·180	− 0·180	− 0·179	− 0·179
0·50	0·0663	0·5215	− 0·158	− 0·158	− 0·160	− 0·161
0·55	0·0617	0·5718	− 0·145	− 0·144	− 0·144	− 0·144
0·60	0·0559	0·6220	− 0·115	− 0·116	− 0·115	− 0·116
0·65	0·0498	0·6723	− 0·098	− 0·099	− 0·093	− 0·093
0·70	0·0433	0·7225	− 0·072	− 0·072	− 0·072	− 0·072
0·75	0·0365	0·7730	− 0·049	− 0·049	− 0·048	− 0·048
0·80	0·0292	0·8235	− 0·024	− 0·025	− 0·023	− 0·023
0·85	0·0218	0·8737	− 0·001	− 0·002	+ 0·005	+ 0·004
0·90	0·0150	0·9239	+ 0·018	+ 0·018	+ 0·024	+ 0·023
0·956	0·0077	0·9801	+ 0·047	+ 0·046	—	—

Radius at Nose $= 0{\cdot}0189$ C.
Radius at Tail $= 0{\cdot}0025$ C.

Table VI.—Values of $(p - p_0)/\rho V_0^2$.

Surface A. $V_0 = 60$ ft./sec. [Uncorrected for the interference of the tunnel walls.]

x/C.	y/C.	$a = 5{\cdot}82°$	$a = 2{\cdot}82°$	$a = -3{\cdot}18°$	$a = -6{\cdot}18°$
0	0	− 0·101	0·377	0·333	− 0·172
0·0002	0·0025	− 0·302	0·275	0·426	+ 0·009
0·0008	0·0050	− 0·509	0·159	0·481	0·195
0·0015	0·0073	− 0·631	+ 0·048	0·504	0·337
0·0027	0·0096	− 0·677	− 0·015	0·507	0·411
0·0039	0·0118	− 0·731	− 0·074	0·501	0·448
0·0053	0·0139	− 0·870	− 0·194	0·481	0·482
0·0069	0·0159	− 0·950	− 0·273	0·457	0·499
0·0085	0·0177	− 1·005	− 0·330	0·420	0·504
0·0103	0·0195	− 1·009	− 0·359	0·396	0·500
0·0167	0·0245	− 0·988	− 0·416	0·310	0·468
0·0330	0·0340	− 0·873	− 0·447	0·168	0·361
0·0504	0·0417	− 0·859	− 0·487	0·069	0·264
0·0756	0·0495	− 0·753	− 0·463	+ 0·007	0·185
0·1007	0·0560	− 0·714	− 0·465	− 0·045	0·122
0·1511	0·0651	− 0·629	− 0·441	− 0·100	0·046
0·2015	0·0707	− 0·556	− 0·400	− 0·116	+ 0·010
0·252	0·0742	− 0·517	− 0·382	− 0·137	− 0·025
0·302	0·0753	− 0·472	− 0·350	− 0·140	− 0·041
0·353	0·0749	− 0·427	− 0·328	− 0·141	− 0·052
0·403	0·0731	− 0·379	− 0·294	− 0·130	− 0·052
0·504	0·0659	− 0·281	− 0·219	− 0·093	− 0·034
0·605	0·0553	− 0·202	− 0·156	− 0·064	− 0·017
0·706	0·0426	− 0·133	− 0·101	− 0·034	0
0·807	0·0281	− 0·060	− 0·040	+ 0·005	+ 0·028
0·868	0·0195	− 0·020	− 0·006	+ 0·027	0·043
0·956	0·0077	+ 0·031	+ 0·040	+ 0·053	0·057

curious waviness in these pressure curves, especially at the nose of the aerofoil. No explanation of this waviness can be offered. There were, however, good reasons to believe that it was not due to local irregularities, or to slight burrs at the edges of the pressure holes, for no irregularities on the metal surface could be detected either by touch or by measurement. Moreover, the waviness was observed on both the upper and lower surfaces, at all speeds and incidences; and also at two sections of surface A. It may be that the waviness arose from general disturbances in the wind of the tunnel, but no attempt was made to determine whether this was the cause.

17. *Form drag.*—The form drag of the aerofoil at $\alpha = -0{\cdot}18°$ was obtained directly from the area* of the diagrams obtained when the values of the pressure coefficient $(p - p_0)/\rho V_0^2$ for each surface were plotted against (y/C). Although a large number of observations (37) was taken on each surface, it

* This area gives the longitudinal force, which can be taken as equal to the drag at an incidence of $-0{\cdot}18°$.

was not possible to determine the form drag very accurately, for the pressure diagrams for each surface consisted of two loops of opposite sign, and the difference between the areas of these loops was small in comparison with the area of either loop. The mean value of K_D obtained from two estimations was 0·00145 for 60 feet per second and also for 80 feet per second. There may be an error between $\pm$ 10 per cent. in this estimated value of K_D. An error of this magnitude in the estimation of the form drag will give an error between $\pm$ 4 per cent. in the predicted value of frictional drag. The pressure data obtained from the experiments were not sufficient to allow the form drag at the incidences 2·82° and 5·82° to be predicted, for at these incidences only the pressure distributions over surface A were measured.

18. *Frictional drag.*—The value of the frictional drag coefficient obtained when the form drag coefficient was subtracted from the total drag coefficient was 0·00395 for the wind speed 60 ft./sec. and the same value for 80 ft./sec. The values of the coefficient of frictional drag obtained from the measured frictional intensities were 0·00425 ($V_0 = 60$) and 0·00435 ($V_0 = 80$) (see Table IV). The differences between the two sets of values are small, and amount to 0·0003 at 60 ft./sec. and 0·0004 at 80 ft./sec. There is therefore a close agreement between the values of the frictional drag obtained by the two entirely different methods. Evidence has therefore been obtained which indicates that, in general, the velocities measured with the small surface tubes are reliable, and also that the assumption made to predict the intensity of the surface friction—that is, that within 2 or 3 thousandths of an inch from the surface the velocity increases at a linear rate from the zero value at the surface—cannot be very far from the truth.

Explorations of Velocity in the Boundary layer ($\alpha = -0{\cdot}18°$).

19. Explorations of velocity were made near the Surface A of the aerofoil at an incidence of $-0{\cdot}18°$ for the two wind speeds 60 and 80 ft./sec. This work was undertaken to obtain some general information on the flow in the boundary layer, that is the thin layer which is retarded by the surface; and also because it was considered necessary to show that the velocities measured very close to the surface with the small surface tubes could be connected in a satisfactory manner with velocities measured at a greater distance from the surface. The additional velocity measurements have also allowed a third prediction of the frictional drag to be made from a consideration of the momentum and pressure changes in the boundary layer.

20. *Velocity experiments.*—The velocity distributions were predicted from

observations of total head taken with two small tubes, hereinafter referred to as Pitots A and B. The smaller Pitot A was used for the explorations made at the front part of the aerofoil, $x = 0{\cdot}052$ C to $0{\cdot}40$ C, and the larger Pitot B for those at the rear part, $x = 0{\cdot}5$ C to $0{\cdot}956$ C. Pitot A was constructed from a short length of fine hypodermic steel tube (external diameter $0{\cdot}0197$ inch), pressed at one end into a rectangular form, of external dimensions $0{\cdot}029$ inch $\times$ $0{\cdot}010$ inch (width). The width of the opening was $0{\cdot}0024$ inch. Pitot B was made from a tube of larger bore; the widths at the mouth being $0{\cdot}0135$ inch (external) and $0{\cdot}0071$ inch (opening). Each tube was mounted with its axis in the tangential direction, and with a longer side of the mouth parallel to the surface. At a distance of about one inch from the mouth, each tube had a right-angle bend, and the stem so obtained passed through a small hole in the aerofoil. This stem was soldered into a stiff cylindrical tube, which in turn was clamped to the screw of a standard micrometer. Attached to the nut of the micrometer was a wheel with 25 teeth, which was turned by a pawl controlled by an electromagnet.* By means of this device mounted within the aerofoil, the exploring tube could be moved outward from the surface in steps of about $0{\cdot}001$ inch.

A preliminary trial of the device showed that the reading of the micrometer scale did not give a sufficiently reliable measure of the distance of a tube from the surface when this distance was small. Calibrations of the micrometer scale were therefore made before and after each exploration of total head by measuring the distance of the centre of the mouth from the surface with a travelling microscope with cross-wires focussed on the mouth. To obtain clear definition, the mouth of the tube and the neighbouring surface was illuminated with a beam of light from a Pointolite lamp.

21. *Calibration of Pitot tubes.*—It is known that the pressure at the mouth of a very small Pitot tube differs from the total head in the airstream impinging on the mouth. Each of the Pitots A and B were therefore calibrated in a uniform wind, for the speed range covered in the aerofoil experiments. The observed values of $(2P/\rho V_0^2)$, where P is the excess of the pressure at the mouth of a Pitot over the total head in the wind, are given in Table VII. It is there seen that the value of P, and so the pressure at the mouth of a tube, depended on whether the speed of the tunnel wind had been raised or lowered to the steady value of observation; and that in general the observations of

* The electromagnet could not be accommodated within the aerofoil at the tail, and it was then necessary to mount the exploring tube on a device carried on the aerofoil surface.

pressure taken when the tunnel speed was raised to its steady value were greater than those taken when it was lowered to the steady value. The mean values of P were, however, small provided the velocity at the mouth of a Pitot was greater than about 30 ft./sec. Since almost all the velocities measured in the aerofoil experiments were greater than 30 ft./sec., it was decided that the corrections to be applied to the observations should be taken from the curves obtained when the mean values of P given in Table VII were plotted against V.

Table VII.—Calibration of Pitots A and B in a uniform wind.

P ≡ excess of the pressure at the mouth of a Pitot over the total head in the wind.

The values given are the means from several calibrations.

Velocity, V, at the mouth of Pitot. ft./sec.	Values of $(2P/\rho V^2)$. Pitot A.	Mean.	Pitot B.	Mean.	
80	(a) 0·020 (b) 0·015	0·018	0·008 0·008	0·008	(a) Tunnel speed slowly raised to its steady value.
60	(a) 0·018 (b) −0·013	0·003	0·007 0·002	0·005	(b) Tunnel speed slowly lowered to its steady value.
40	(a) 0·028 (b) −0·030	−0·001	0·011 0·004	0·008	
22·5	(a) 0·040 (b) −0·096	−0·028	0·039 −0·028	0·006	

To determine to what extent the Pitots were suitable for observation in a region of steep velocity gradient, such as that near a surface, observations were taken with Pitot A mounted in the laminar flow adjacent to a wall of the pipe used in the earlier experiments described in § (8). The velocity gradient at thewall of the pipe was such that the theoretical velocity at the outer edge of the Pitot mouth was about 50 per cent. greater than that at its centre. The results of the calibration are given in Table VIII. They show that provided the velocity calculated from the pressure at the mouth exceeded 26·8 ft./sec. —the minimum velocity measured with the Pitot in the boundary layer of the aerofoil was about 30 ft./sec.—the effective centre was situated at a constant distance of about 0·0054 inch from the wall. The effective centre was therefore situated at a lateral distance of about 0·0005 inch from the

Table VIII.—Observations taken with Pitot A in the laminar flow at the wall of a pipe.

$\bar{z}$ = distance of effective centre from wall.

V = velocity calculated from the pressure at the mouth of the Pitot tube.

Distance of the geometrical centre of the Pitot mouth from the wall was 0·0059 inch.

V. ft./sec.	*Theoretical* velocity at the outer edge of Pitot mouth.	$\bar{z}$ inches.
48·9	75·0	0·0053
37·5	56·8	0·0053
31·6	47·3	0·0054
26·8	39·6	0·0055

oint ($z = 0{\cdot}0059$ inch) which was taken as the geometrical centre of the outh.* No corrections for "wall" interference were applied to the bservations taken on the aerofoil with either Pitot A or B. The results in able VIII indicate then that a small error in z of about 0·0005 inch is ossible when a tube is touching the surface. Any error in z should, however, apidly decrease as the distance from the surface is increased.

22. *Velocity results.*—Explorations of total head (time-average values) were ade in the boundary layer, along 12 lines normal to surface A. The first xploration was at $x = 0{\cdot}0524$ C and the twelfth at $x = 0{\cdot}956$ C. The wind peeds were 60 and 80 ft./sec. The incidence of the aerofoil was $-0{\cdot}18°$. he velocity distributions were estimated from the total-head explorations orrected as described in § 21) on the assumption that the static pressure long each normal line was constant and equal to the value measured at the rface.

The velocity coefficients (V/V_0) obtained with the Pitot tubes A and B are lotted (as dots) against (z/C), at a constant value of (x/C), in figs. 10 and 11. These points are seen to lie closely on smooth curves. The results obtained in § 10 with the small surface tubes are also plotted in figs. 10 and 11. These results are seen to lie very closely on the curves drawn through the results obtained with the Pitots A and B. The two sets of results are therefore compatible.

* Some small uncertainty in the position of the geometrical centre existed, owing to irregularities in the shape of the mouth.

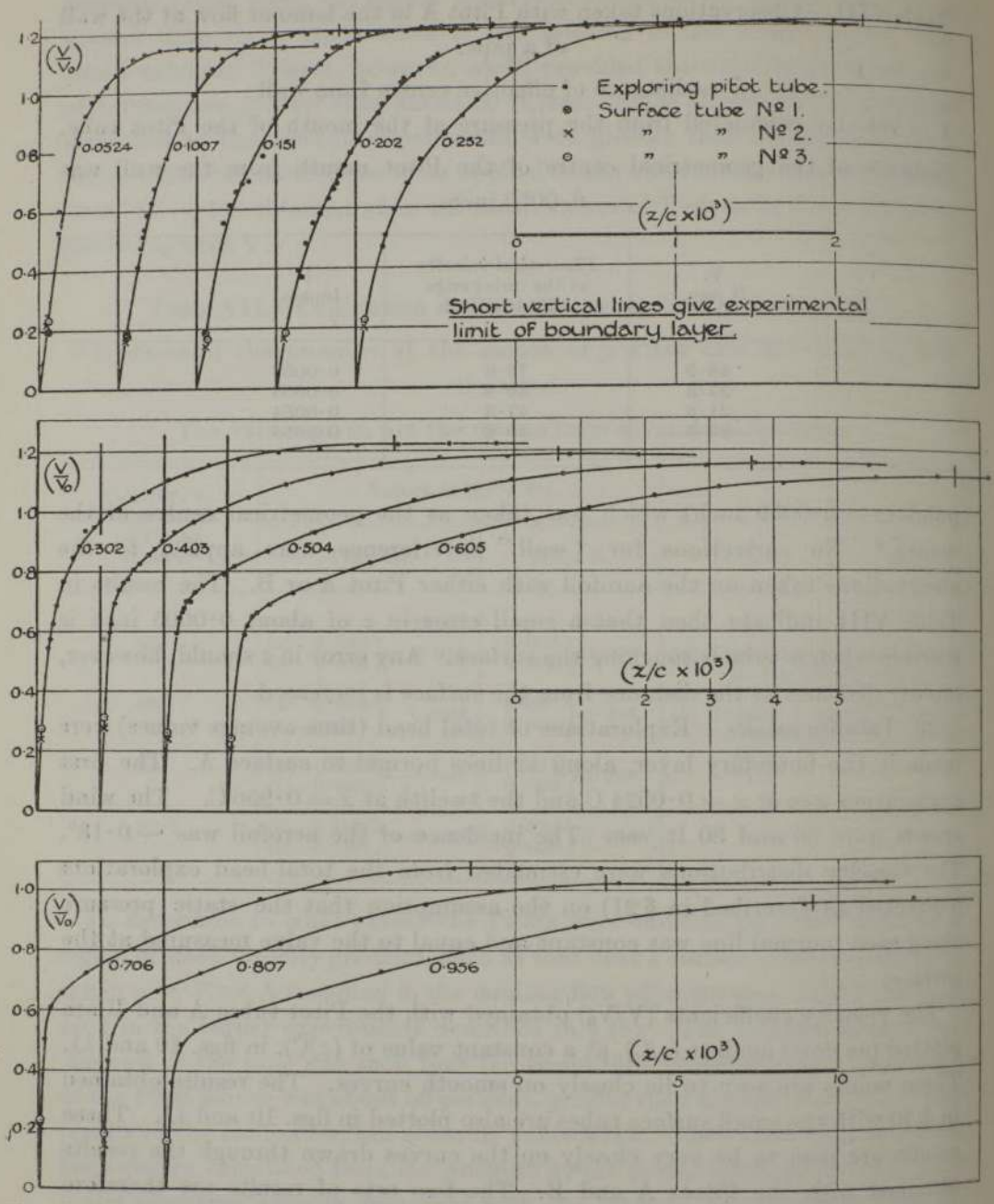

FIG. 10.—Velocity Distribution in Boundary Layer. Surface A, $\alpha = -0{\cdot}18°$ $V_0 = 80$ ft./sec. Values of x/C given on curves.

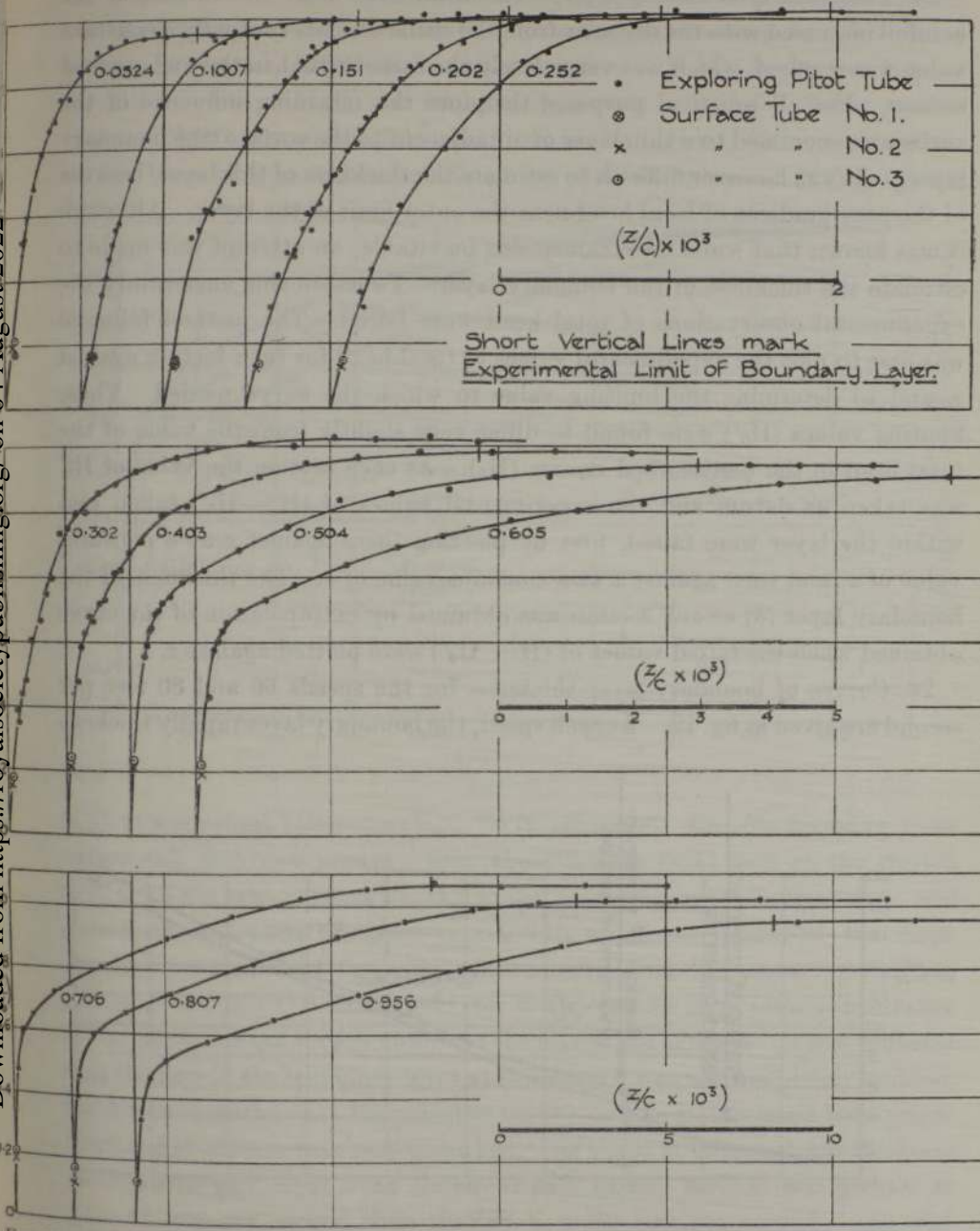

Fig. 11.—Velocity Distribution in Boundary Layer. Surface A, $\alpha = -0{\cdot}18°$ $V_0 = 60$ ft./sec. Values of x/C given on curves.

23. *Thickness of boundary layer.*—The total head near the surface of the aerofoil increased with the distance from the surface until eventually a constant value was reached, which was very closely the same as that in the undisturbed stream. For all practical purposes therefore the retarding influence of the surface was confined to a thin layer of air adjacent to the surface (the boundary layer). It was however difficult to estimate the thickness of this layer, because of the easy gradient of total head near the outer limit of the layer. Although it was known that some uncertainty was inevitable, an attempt was made to estimate the thickness of the boundary layer. To lessen this uncertainty the experimental observations of total head were faired. The method followed was first to plot the experimental values of total head for each section against z, and to determine the limiting value to which the curve tended. These limiting values (H_0') were found to differ very slightly from the value of the total head in the undisturbed stream (H_0). At each section the value of H_0' was taken as datum and the experimental values of $(H - H_0')$ taken just within the layer were faired, first by plotting them against z at a constant value of x, and then against x at a constant value of z. The thickness of the boundary layer (δ) at any section was obtained by extrapolation of the curve obtained when the faired values of $(H - H_0')$ were plotted against z.

24. Curves of boundary-layer thickness for the speeds 60 and 80 feet per second are given in fig. 12. At each speed, the boundary layer rapidly thickens

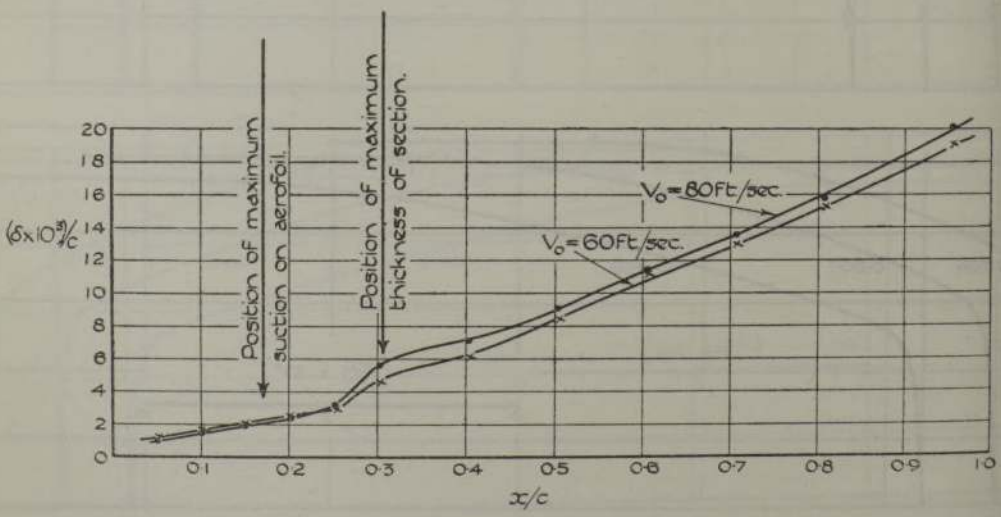

Fig. 12.—Thickness of Boundary Layer.

between the regions of maximum suction and of maximum thickness. This rapid thickening is a common feature of the flow in a boundary layer and, in

the absence of a breakaway or a sudden change of curvature of the surface, marks the region where a transition from laminar to turbulent flow takes place. It appears then that the transition ($\alpha = -0{\cdot}18°$) began just beyond $x = 0{\cdot}25\,C$ and that it was completed near $x = 0{\cdot}35\,C$. Some general evidence that a transition of flow occurred in this region is given in the curves of fig. 13, which have been obtained by plotting values of (V/V_0) against

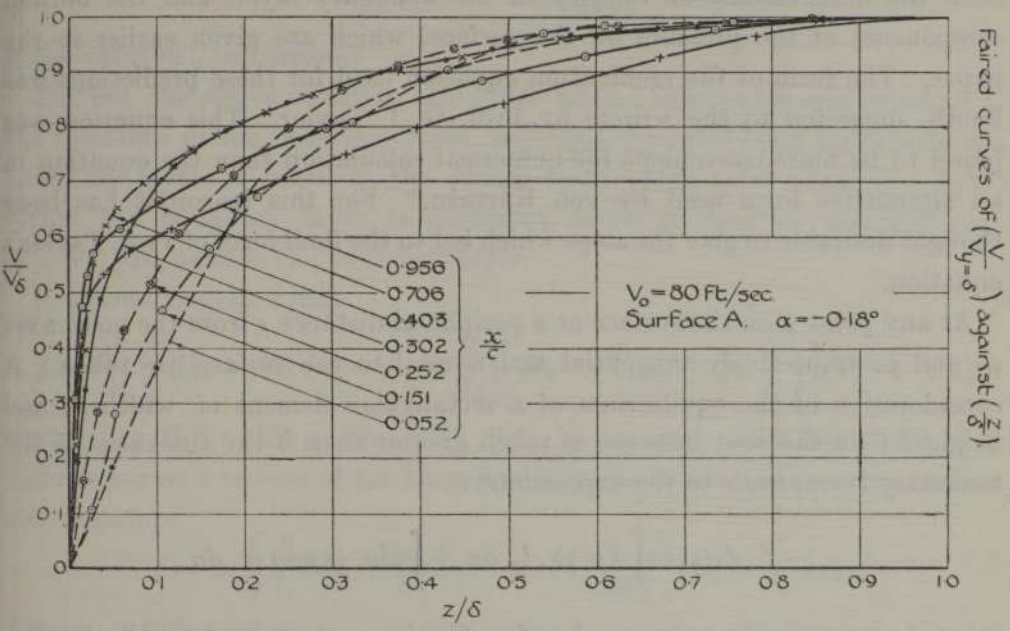

FIG. 13.

(z/δ), at a constant value of x ($V_0 = 80$ ft. per sec.)*. Broadly speaking, these curves fall into two groups; first, those for the front part of the surface ($x < 0{\cdot}25\,C$), which resemble the shape associated with laminar flow, and second, those for the rear part ($x > 0{\cdot}3\,C$) which are typical of the shape obtained for turbulent flow. It will be noted that the curve for the first section $x = 0{\cdot}052\,C$ is rather odd, for it appears to have some resemblance to the curves for the turbulent flow at the rear of the aerofoil. It was probable that the flow in the boundary layer at this section was not completely laminar, for it was observed that the pressure on the surface in the immediate neighbourhood of the nose was very disturbed. As would be expected, the thickness of the boundary layer over the front part of the aerofoil was greater at $V_0 = 60$ feet per second than that at $V_0 = 80$ feet per second; and also the transition occurred later at the lower speed. It will be observed that there was no indication of any rapid thickening of the boundary layer near

* The curves for $V_0 = 60$ ft./sec. ($\alpha = -0{\cdot}18°$) showed similar characteristics.

the tail, such as would have occurred if the layer had separated from the surface.

25. *Estimation of the surface friction from the momentum in the boundary layer.*—The changes of momentum in the boundary layer as it flows around the aerofoil are directly related to the normal and tangential components of the pressure on its surface. The surface friction can therefore be predicted from the observations of velocity in the boundary layer, and the normal components of the pressure on the surface, which are given earlier in the paper. The form of the momentum equation used for these predictions was kindly suggested to the writers by Prof. G. I. Taylor. This equation was found to be more convenient for numerical calculation than the equation in an alternative form used by von Kármán.* For this reason it has been thought desirable to give the steps which led to the final form of Prof. Taylor's equation.

At any point p on the surface at a peripheral distance s from the nose, axes ps and pz respectively tangential and normal to the surface are taken. A consideration of the equilibrium of a rectangular element of width ds and height z (z in the first instance is taken greater than δ the thickness of the boundary layer) leads to the expression† :—

$$-f \,.\, ds/\rho = \int_c (p/\rho) \,.\, l \,.\, d\sigma + \int_c (lu + mv)\, u \,.\, d\sigma \,.$$

where f represents the intensity of surface friction, p the pressure, ρ the density, u and v the tangential and normal components of velocity, and (l, m) the direction cosines of the normal to an element $d\sigma$ of the contour of the element. The integrations are taken around the contour c. The expression is then recast into the form,

$$-f \,.\, ds = \int_c (p + \tfrac{1}{2}\rho V^2)\, l \,.\, d\sigma + \int_c \rho \left\{ mvu + l\left(\frac{u^2}{2} - \frac{v^2}{2}\right)\right\} d\sigma,$$

where $V^2 = u^2 + v^2$.

Neglecting v^2 and writing $v_z = -\, d/ds \int_0^z V dz$, the above expression becomes

$$-f = \frac{d}{ds}\int_0^z (p + \tfrac{1}{2}\rho V^2)\, dz - \rho V_z \,.\, \frac{d}{ds}\int_0^z V dz + \tfrac{1}{2}\rho \frac{d}{ds}\int_0^z V^2 dz.$$

* 'Z. Angew. Math. Phys.,' vol. 1 (1921).

† See G. I. Taylor. 'Phil. Trans. Roy. Soc.,' A, vol. 225, p. 239.

It then follows that

$$-f = \frac{d}{ds}\int_0^z (p + \tfrac{1}{2}\rho V^2)\,dz - \rho V_z \frac{d}{ds}\int_0^z (V - V_z)\,dz + \tfrac{1}{2}\rho \frac{d}{ds}\int_0^z (V^2 - V_z^2)\,dz,$$

since

$$\left[-V_z\rho \frac{d}{ds}\int_0^z V_z\,dz + \tfrac{1}{2}\rho \frac{d}{ds}\int_0^z V_z^2\,dz\right] = 0,$$

if the value of $_z$ be constant.

Further, the above equation also holds when $_z$ is variable and equal to δ, the thickness of the boundary layer, provided the total head H_0 outside the boundary layer be taken as the datum from which total head $(p + \frac{1}{2}\rho V^2)$ within the boundary layer is measured, since it may be assumed that $(V = V_\delta)$ just outside the boundary layer.

It follows therefore that

$$f = \frac{d}{ds}\int_0^\delta (H_0 - H)\,dz - \rho\,.\,V_\delta \frac{d}{ds}\int_0^\delta (V_\delta - V)\,dz + \tfrac{1}{2}\rho \frac{d}{ds}\int_0^\delta (V_\delta^2 - V^2)\,dz.$$

Further $\frac{1}{2}\rho\ (V_\delta^2 - V^2) = (H_0 - H)$, if it be assumed that the pressure is uniform across a section of the boundary layer and the same as at the surface and therefore

$$f = 2\frac{d}{ds}\int_0^\delta (H_0 - H)\,dz - \rho\,.\,V_\delta\,.\,\frac{d}{ds}\int_0^\delta (V_\delta - V)\,.\,dz.$$

Finally, it follows that

$$\int_0^s f\,.\,ds = 2\int_0^\delta (H_0 - H)\,dz - \int_0^s V_\delta\,.\,dM_1,$$

where

$$M_1 = \int_0^\delta \rho\,(V_\delta - V)\,dz.$$

26. Since the velocity values given in figs. 10 and 11 were determined from the observations taken when the total head was measured directly against the pressure at the surface, it follows from the method of derivation of the above equation for $\int_0^s f\,ds$, that the datum total head* must be the value measured just outside the layer. Values of $\int_0^s f\,.\,ds$ calculated in this manner from the experimental data taken at the wind speeds 60 and 80 ft./sec. are plotted against s in fig. 14. The values obtained from the integral of the

* The datum total head measured just outside the layer occasionally differed very slightly from the total head in the undisturbed stream.

frictional intensities given in Table II are also plotted in this figure. The curves drawn through the two series of points are seen to lie fairly close

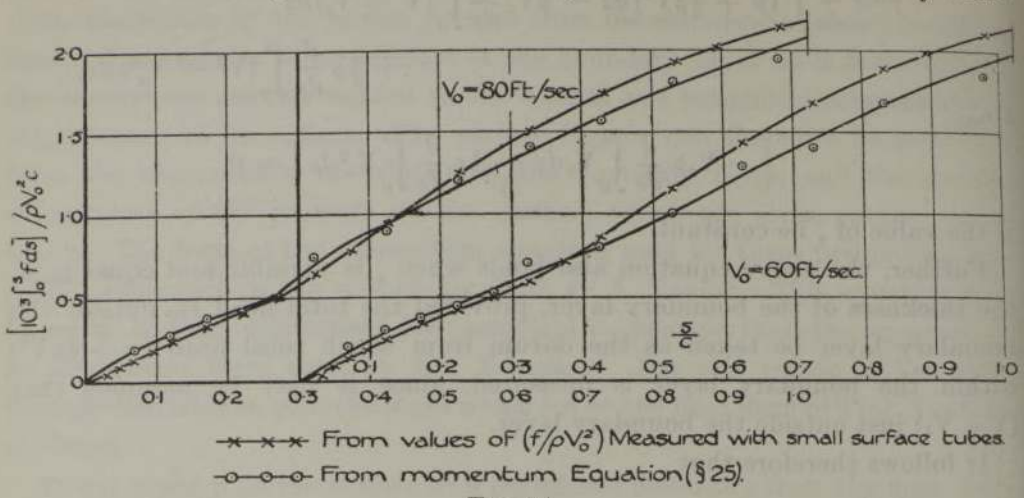

FIG. 14.

together, except near the nose, at sections $s = 0{\cdot}068$ C and $0{\cdot}120$ C. That there were differences at these sections is not surprising, for the value of $\int_0^s V_\delta dM_1$ for the section $s = 0{\cdot}068$ C had to be obtained by extrapolation, for no measurements of velocity were made in the boundary layer forward of this section. Also it is not certain that the condition assumed in the derivation of the momentum expression, namely, that the static pressure at all points in a section of the boundary layer is uniform and the same as that at the surface, holds with sufficient accuracy at the nose, since the curvature of the surface is rapidly changing in this region. It is of interest to mention here that observations taken in the section $x = 0{\cdot}956$ C at the tail showed that the static pressure within the boundary layer was constant and the same as that at the surface.

27. It is shown in § 13 that at $\alpha = -0{\cdot}18°$ the drag of the aerofoil obtained from the intensities of surface friction was only 2 per cent. smaller than the sum of the values of $\int_0^s f\,.\,ds$ for the two surfaces. The values of $\int_0^s f\,.\,ds$ for the surface A obtained from the momentum equation of § 25 were $0{\cdot}00209\ \rho CV_0^2$ (80 ft./sec.) and $0{\cdot}00200\rho CV_0^2$ (60 ft./sec.). Since at $\alpha = -0{\cdot}18°$ the value of $\int_0^s f\,.\,ds$ for surface B can be taken as the same as that for Surface A, the values of K_D (frictional) are $0{\cdot}00410$ (80 feet per second) and $0{\cdot}00390$ (60

feet per second). These values of K_D are compared in Table IX with those obtained in § (13) from the frictional intensities measured with the small surface tubes and those obtained in § (18) from the measurements of the total and form drags. The three series of results are seen to be in reasonably close agreement. In general, then, the accuracy of the experimental work described in the paper is satisfactory.

Table IX.—Values of K_D (frictional). $\alpha = -0{\cdot}18°$.

Source of Results.	$V_0 = 60$ ft./sec.	$V_0 = 80$ ft./sec.
From observations taken with the small surface tubes. § (13)	0·00425	0·00435
From measurements of total drag and form drag § (18)	0·00395	0·00395
From observations of velocity in boundary layer. (Momentum Equation.) § (25)	0·00390	0·00410

28. *Details of aerofoil section.*—The section was derived from a circle by a conformal transformation of the generalised Joukowski type given by the expression $(\zeta - nc)/(\zeta + nc) = (z - c)^n/(z + c)^n$. An outline of the method of calculating the shape is given in the paper referred to earlier in § (15). The values of the shape parameters were $(a/c) = 1{\cdot}10$ and $n = 1{\cdot}95$. This theoretical section had a tail which tapered gradually to a sharp edge; and since this was a shape which could not be reproduced with great accuracy on the model, a small part of the tail was cut off and the shape completed by rounding off the trailing edge. The chord length of the theoretical shape was 40·52 inches, and that of the section used in the experiments 39·7 inches. The maximum thickness was 5·98 inches and occurred at one-third of the chord.

As mentioned earlier in § 2, the central part of the aerofoil of span 6 inches was cut from a hollow gunmetal casting. The shape of surface A of the finished model was checked on a milling machine before the experiments were commenced. It was found that the shape from the nose to the maximum ordinate agreed, within the accuracy of measurement, with the theoretical shape, but that there was a small difference from the theoretical shape over the region $x = 18$ inches to 27 inches. The maximum difference occurred at about $x = 22{\cdot}5$ inches, and was such that the actual value of y was about 0·996 of its theoretical value. Only the contours for the theoretical shape have been given in the paper (Table V), for it is unlikely that the small departure of the

actual shape from the theoretical shape, which occurs just beyond the maximum thickness, will effect to any measurable extent the flow around the surface.

29. *Summary.*—The intensity of friction over the surface of a large symmetrical aerofoil of the Joukowski type (chord 39·7 inches) has been determined from measurements of velocity taken very near the surface with small surface tubes of the Stanton type. The characteristic feature of this type of tube is that the inner wall of the tube is formed by the surface itself. Three tubes with openings 0·0020, 0·0032 and 0·0044 inch respectively were used. These tubes allowed measurements of velocity to be taken at distances of 0·002 to 0·003 inch from the surface.

The velocity gradients at the surface $(\partial V/\partial z)_{z=0}$ were determined from these velocity measurements, and the intensities of the surface friction (f) from the well-known relation $f = \mu\,(\partial V/\partial z)_{z=0}$.

The results obtained showed that on each surface the frictional intensity had a maximum value at a short distance from the nose, and a second and larger maximum value just beyond the first. As the incidence was increased (0° to 6°), the maximum values on the upper surface increased and moved nearer the nose, whereas those on the lower surface decreased slightly and moved towards the tail. The first maximum value was associated with laminar flow, and the second with turbulent flow in the boundary layer.

Measurements of velocity in the boundary layer were also made with small exploring tubes, and these measurements were found to be compatible with those made nearer the surface with the surface tubes.

Evidence on the general accuracy of the values of the frictional intensity was obtained from a comparison of the frictional drag of the aerofoil estimated from them with values obtained by two other methods. In the first method, the frictional drag was determined by subtracting the form drag, obtained from the normal pressures on the surface, from the total drag estimated from the total-head losses in the wake; and in the second, the frictional drag was estimated from an equation derived from a consideration of the momentum and pressure changes in the boundary layer. The values of the frictional drag obtained by the three different methods were found to be in reasonably close agreement.

30. In conclusion, the authors wish to express their great indebtedness to Messrs. J. H. Warsap and C. Scruton, who assisted in the experimental work; to Mr. A. Monk, who made the metal aerofoil and the exploring Pitot tubes; and to Mr. J. Barber, who successfully overcame the great difficulties involved in the construction of the small surface tubes.